Replacement or exclusion of the B-branch bacteriopheophytin in the purple bacterial reaction centre: The H$_B$ cofactor is not required for assembly or core function of the *Rhodobacter sphaeroides* complex

Ashley J. Watson [a], Paul K. Fyfe [a,1], Dmitrij Frolov [b], Marion C. Wakeham [a], Eliane Nabedryk [c], Rienk van Grondelle [b], Jacques Breton [c], Michael R. Jones [a,*]

[a] *Department of Biochemistry, School of Medical Sciences, University of Bristol, University Walk, Bristol, BS8 1TD, UK*
[b] *Department of Physics and Astronomy, Free University of Amsterdam, De Boelelaan 1081, 1081, HV, Amsterdam, The Netherlands*
[c] *Service de Bioénergétique, Bâtiment 532, CEA Saclay, 91191 Gif-sur-Yvette Cedex, France*

Abstract

All of the membrane-embedded cofactors of the purple bacterial reaction centre have well-defined functional or structural roles, with the exception of the bacteriopheophytin (H$_B$) located approximately half-way across the membrane on the so-called inactive- or B-branch of cofactors. Sequence alignments indicate that this bacteriochlorin cofactor is a conserved feature of purple bacterial reaction centres, and a pheophytin is also found at this position in the Photosystem-II reaction centre. Possible structural or functional consequences of replacing the H$_B$ bacteriopheophytin by bacteriochlorophyll were investigated in the *Rhodobacter sphaeroides* reaction centre through mutagenesis of residue Leu L185 to His (LL185H). Results from absorbance spectroscopy indicated that the LL185H mutant assembled with a bacteriochlorophyll at the H$_B$ position, but this did not affect the capacity of the reaction centre to support photosynthetic growth, or change the kinetics of charge separation along the A-branch of cofactors. It was also found that mutation of residue Ala M149 to Trp (AM149W) caused the reaction centre to assemble without an H$_B$ bacteriochlorin, demonstrating that this cofactor is not required for correct assembly of the reaction centre. The absence of a cofactor at this position did not affect the capacity of the reaction centre to support photosynthetic growth, or the kinetics of A-branch electron transfer. A combination of X-ray crystallography and FTIR difference spectroscopy confirmed that the H$_B$ cofactor was absent in the AM149W mutant, and that this had not produced any significant disturbance of the adjacent ubiquinol reductase (Q$_B$) site. The data are discussed with respect to possible functional roles of the H$_B$ bacteriopheophytin, and we conclude that the reason(s) for conservation of a bacteriopheophytin cofactor at this position in purple bacterial reaction centres are likely to be different from those underlying conservation of a pheophytin at the analogous position in Photosystem-II.
© 2005 Elsevier B.V. All rights reserved.

1. Introduction

The *Rhodobacter* (*Rb.*) *sphaeroides* reaction centre is a membrane-spanning electron transfer complex composed of three polypeptides, termed H, L and M, that encase ten cofactors. These are four molecules of bacteriochlorophyll *a* (BChl *a*), two molecules of bacteriopheophytin *a* (BPhe *a*), two molecules of ubiquinone, a single photoprotective carotenoid and a non-heme iron atom. BChl *a* and BPhe *a* are identical molecules, with the exception that the central magnesium atom of the former is replaced by two hydrogen ions in the latter, a difference that affects the absorbance and

electrochemical properties of the cofactor, its ligation to the protein, and its stability and reactivity. The L- and M-polypeptides each have five membrane-spanning α-helices, and these are arranged around an axis of two-fold rotational pseudo-symmetry that runs perpendicular to the plane of the membrane, forming a heterodimeric protein scaffold that encases the BChl, BPhe and ubiquinone cofactors [1–5]. At the periplasmic side of the membrane, two BChls (P_A and P_B) are arranged as an excitonically-coupled dimer (termed P) that straddles the symmetry axis (Fig. 1). The remaining BChl (B_A, B_B), BPhe (H_A, H_B) and ubiquinone (Q_A, Q_B) cofactors are arranged in two approximately symmetrical branches that connect the P dimer with the cytoplasmic side of the membrane (Fig. 1). Breaking this symmetry, the single carotenoid is embedded in the M-polypeptide, adjacent to B_B [1–5].

In the initial steps of energy transduction, light energy drives a transmembrane electron transfer from the P dimer to Q_A [6–10]. This electron transfer takes place on a picosecond time-scale, and is generally agreed to be a three-step process involving the intervening B_A and H_A bacteriochlorins. The system progresses through three radical pair states, the light-activated singlet excited state of P (P^*) leading to $P^+B_A^-$, then $P^+H_A^-$ and then $P^+Q_A^-$ [7–10]. The electron residing on the Q_A ubiquinone is then passed to the Q_B cofactor binding site, where a bound ubiquinone is reduced to the ubisemiquinone [11,12]. A second light-driven transmembrane electron transfer results in a second reduction and double protonation of the Q_B ubisemiquinone to form ubiquinol [11,12].

Most of the reaction centre cofactors have a well-defined functional role. The P, B_A and H_A bacteriochlorins and Q_A and Q_B ubiquinones participate in light-driven electron transfer and ubiquinol formation. The non-heme iron plays a structural role

at the interface of the L- and M-polypeptides, between the Q_A and Q_B sites, and there is speculation as to whether it plays a role in electron transfer from Q_A^- to Q_B. The carotenoid, spheroidene or spheroidenone in *Rb. sphaeroides*, depending on growth conditions [13], has the potential to act as an accessory light harvesting pigment [14,15], but its primary role is probably the quenching of potentially harmful BChl triplet excited electronic states that can form in reaction centres when forward electron transfer is blocked [13,16,17]. The risk posed by these states, which are sufficiently energetic and long-lived to sensitise singlet oxygen, is countered by triplet energy transfer to the carotenoid, which has a much lower triplet state energy [13]. The B_B BChl appears to play a role in the transfer of triplet state energy from the P BChls to the photoprotective carotenoid [18–27], and transfer of singlet state energy from the carotenoid to P [15,28].

The cofactor for which there is no obvious role is the BPhe at the H_B position. It is needed to maintain the structural symmetry of the reaction centre, and to complete the B-branch of cofactors, but this branch is thought not to play a significant role in transmembrane electron transfer, and the mechanism of the purple bacterial reaction centre is based on asymmetry, with specialised roles for the A- and B-sides. This raises the question of why the complex has evolved to show strong functional asymmetry, but has nevertheless retained marked structural symmetry.

One possible answer is that retention of the H_B cofactor is required to provide structural stability [29]. BPhe is a large molecule, with a tetrapyrrole head-group and a long hydrocarbon side chain, and it is conceivable that loss of such a large cofactor could destabilise the reaction centre, or cause problems during assembly. However this would not explain
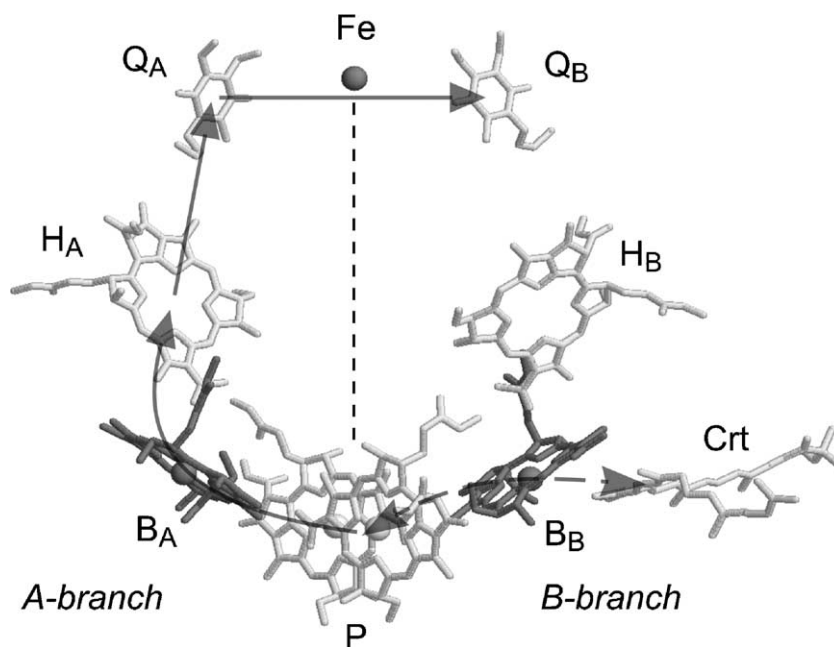
Fig. 1. Cofactor organisation in the *Rb. sphaeroides* reaction centre. The BChl, BPhe and ubiquinone cofactors are arranged around an axis of two-fold symmetry (dotted line) in two branches that span the membrane. The hydrocarbon side chains of these cofactors have been removed for clarity, and the accessory BChls are highlighted in dark grey. The route of light-driven electron transfer from P to Q_B is shown by the solid arrows. The route of triplet energy transfer from P to the carotenoid and singlet energy transfer in the reverse direction is shown by the dashed double-headed arrow.

why H_B has been retained as a BPhe, rather than the more abundant BChl that is found elsewhere in the bacterial photosynthetic apparatus. In wild-type *Rb. sphaeroides* strains, the reaction centre is surrounded by BChl-containing antenna pigment–protein complexes that feed the reaction centre with excitation energy, but it is thought that BPhe *a* is exclusive to the H_A and H_B positions in the reaction centre. On the A-branch of cofactors, the fact that H_A is a BPhe ensures that there is a free energy drop on transition from the $P^+B_A^-$ to $P^+H_A^-$ state (as BPhe *a* is easier to reduce than BChl *a* by some 200–300 mV). This contributes to the rate and efficiency of membrane-spanning electron transfer along the A-branch, and the high quantum yield with which the complex operates. However, from a purely structural standpoint there seems to be no reason why the unusual BPhe cofactor should be retained at the H_B position.

The most obvious functional properties that distinguish BPhe *a* from BChl *a* are its blue-shifted absorbance spectrum and lower reduction potential. It is therefore conceivable that H_B is a BPhe to ensure efficient (energetically-downhill) energy transfer from H_B to the B_B BChl, maximising light harvesting, or to ensure that any electron transfer along the B-branch from P to Q_B is highly efficient, maximising quantum yield. Another possibility, proposed recently by Woodbury and co-workers, is that the H_B BPhe participates in a photoprotective charge separation in response to near-ultraviolet or blue light excitation of the reaction centre, through formation of the charge separated state $B_B^+H_B^-$ [30,31].

In the present report, site-directed mutagenesis has been used to examine the consequences of replacing BPhe with BChl at the H_B site, through mutagenesis of Leu L185 to His (LL185H). This follows the lead provided by the symmetrical Leu M214 to His (LM214H) mutation on the A-branch, which causes a BChl to be incorporated at the H_A position in place of the native BPhe [32–34]. In addition, following the example provided by the mutation Ala M260 to Trp (AM260W), which leads to steric exclusion of the Q_A ubiquinone from the reaction centre [35,36], we have introduced an Ala to Trp mutation into the binding pocket of the H_B cofactor at position M149. The spectroscopic properties and X-ray crystal structure of the resulting AM149W mutant show that the reaction centre can assemble without a bacteriochlorin in the H_B binding pocket. The functional consequences of this H_B-excluding mutation are examined.

2. Materials and methods

2.1. Mutagenesis and bacterial strains

All mutations were generated using the QuikChange mutagenesis kit (Stratagene). The template was plasmid pUCXB-1, which is a derivative of pUC19 containing a 1841-bp *Xba*I–*Ba*mHI restriction fragment encompassing *pufLM* [37]. Mutagenic changes were confined to the target codon and were confirmed by DNA sequencing. Reaction centre *pufLM* genes containing these mutations were expressed in *Rb. sphaeroides* deletion strain DD13 [38], using a derivative of expression vector pRKEH10D that lacks the *pufBA* genes that encode the core LH1 antenna complex [38]. This produced transconjugant strains that had mutant reaction centres but lacked both the LH1 and LH2 light-harvesting complex (an $RC^+LH1^-LH2^-$ phenotype). Mutated *pufLM* genes

were also expressed in deletion strains DD13 and DPF2 using a derivative of expression vector pRKEH10 [38], producing transconjugant strains with a $RC^+LH1^+LH2^-$ or $RC^+LH1^+LH2^+$ phenotype, respectively.

2.2. Preparation of intracytoplasmic membranes and purified reaction centres

Experimental material for steady-state and time-resolved absorbance spectroscopy consisted of intracytoplasmic membrane fragments prepared from cells that had been grown under semiaerobic conditions in the dark, using procedures described previously [39]. For the preparation of reaction centres, membrane fragments were suspended in 20 mM Tris–HCl (pH 8.0) and reaction centres were solubilised by the addition of NaCl to 100 mM followed by lauryl dimethylamine oxide (LDAO) to 1.5%. Solubilised reaction centres suspended in 20 mM Tris–HCl/0.1% LDAO (pH 8.0) were purified by two sequential passes through a DE52 anion exchange column, followed by passage through Sepharose Q and Sephadex 200 columns (Pharmacia), as described in detail elsewhere [37].

2.3. Spectroscopy

Room temperature absorbance spectra of intracytoplasmic membranes diluted in 20 mM Tris–HCl (pH 8.0) were recorded using a Beckman DU640 spectrophotometer. To ensure full reduction of the P BChls, spectra were recorded in the presence of 1 mM sodium ascorbate and 25 μM phenazine methosulphate (PMS). 77 K absorbance spectra of intracytoplasmic membranes were recorded using a Perkin Elmer Lambda 40 UV-VIS double beam spectrophotometer and an Oxford Instruments liquid nitrogen cryostat.

Steady-state light-induced Q_B^-/Q_B Fourier transform infrared (FTIR) difference spectra were recorded at 290 K using a Nicolet 860 FTIR spectrometer equipped with a MCT-A detector, a KBr beam-splitter and a cryostat. Each sample of purified wild-type or mutant reaction centres was reconstituted under argon with ten-fold excess of ubiquinone-3 (Q_3), as described previously [40,41] and partially dried under argon on a CaF_2 window. Each sample was covered with 2 μl of a solution containing 100 mM potassium ferrocyanide and 10 mM sodium ascorbate in Tris–HCl buffer (100 mM, pH 7) and was sealed with a second CaF_2 window, yielding a reaction centre concentration of 0.2–0.5 mM. The infrared absorbance at the peak of the amide I band (~ 1655 cm^{-1}) was kept below 0.8 absorbance units. The Q_B^- state was generated upon excitation under low intensity continuous illumination, as described previously [42]. Cycles of illumination were repeated several hundred times, with a delay between cycles to allow near-to-complete relaxation of the light-induced charge separated state. In all experiments, the characteristics of the FTIR spectrum did not change over the course of the experiment, demonstrating that there was no detectable degradation of the sample.

Femtosecond transient absorbance difference spectra were recorded using antenna-deficient membranes, and a spectrometer that has been described previously [43,44]. In brief, the output of a Ti:Sapphire oscillator was amplified by means of chirped pulse amplification (Alpha-1000 US, B.M. Industries) generating 1 kHz, 795 nm, 60 fs pulses. The absorption of the sample was 0.6 OD mm^{-1} at 795 nm, and typically 20% of the reaction centres were excited with each pulse. Transient absorption spectra were collected with probe and excitation beams oriented at the magic angle (54.7°). The steady state absorption spectrum of the sample before and after measurements did not show any changes. Spectra were corrected for white light group velocity dispersion and instrument response function, and fitted globally with five components as described previously [45].

2.4. X-ray crystallography

Trigonal crystals of the AM149W reaction centre, space group P3$_1$21, were grown by sitting drop vapour diffusion as described previously [37]. Briefly, well solutions containing 9 mg ml^{-1} of the AM149W reaction centre, 0.09% v/v LDAO, 3.5% w/v heptane-1,2,3-triol and 0.7 M potassium phosphate (pH 8.0) were equilibrated against a reservoir solution of 1.4 M potassium phosphate. Crystals appeared within 1–2 weeks and presented as prisms of variable size.

Table 1
Crystallographic statistics for data collection and partial refinement

Collection statistics	AM149W reaction center
Resolution range	16.0–3.40 Å
No. of unique observations	24,163
Completeness[a]	83.7% (88.1%)
R_{merge}[b]	10.8% (34.1%)
Refinement statistics	
R_{cryst}[c]	24.7%
R_{free}[d]	29.2%

[a] Figures within brackets refer to the statistics for the outer resolution shell (3.52–3.40 Å).

[b] $R_{merge} = \sum_h \sum_i |<I(h)> - I(h)_i| / \sum_h \sum_i I(h)_i$ where $I(h)$ is the intensity of reflection h, $\sum_h$ is the sum over all reflections, $\sum_i$ is the sum over all i measurements of reflection h.

[c] R_{cryst} is defined by $\sum ||F_O| - |F_C|/\sum|F_O|$.

[d] R_{free} was calculated with 5% reflections selected to be the same as in the refinement of the wild-type reaction center [37].

X-ray diffraction data were collected using cryo-cooled crystals and an ADSC Quantum 4 detector, on beam-line 14.1 of the Daresbury Synchrotron Facility, U.K. Crystals were prepared for cryo-cooling by sequential soaking in mother liquor containing increasing concentrations of ethylene glycol to give a final concentration of 25%. The cryocooled crystals of the AM149W reaction centre had unit cell dimensions of $a = b = 139.3$ Å, $c = 184.4$ Å, $\alpha = \beta = 90°$, $\gamma = 120°$, compared to values from room temperature data on the wild-type reaction centre of $a = b = 142.4$ Å, $c = 188.6$ Å, $\alpha = \beta = 90°$, and $\gamma = 120°$ [37]. The crystal used for data collection diffracted to a higher resolution limit of 3.4 Å, and diffraction data were processed and scaled using HKL2000 [46]. Molecular replacement was performed using AMORE [47] using the coordinates of the wild-type reaction centre as the search model [37]. Rigid body refinement was carried out before partial refinement using restrained maximum likelihood refinement in REFMAC 5.0 [48]. Modelling of the area surrounding the H_B binding site was carried out on the basis of omit maps, with the H_B BPhe absent in the initial round of refinement. The M149 residue was retained as alanine in this initial round of refinement because alanine has the smallest aliphatic side-chain. Data collection and refinement statistics are given in Table 1.

3. Results

3.1. Is the H_B BPhe completely conserved?

Before embarking on mutagenesis studies, we first looked for evidence that the H_B BPhe is in fact a completely conserved feature of the purple bacterial reaction centre. Although reaction centres from only a few species have been characterised by spectroscopy or X-ray crystallography, protein sequence information is available for the L- and M-polypeptides from over 40 species of purple bacteria. Accordingly, we looked at sequence conservation of key amino acids lining the H_A and H_B binding pockets to assess whether these cofactors are always present as BPhes. This was done by analysing an alignment of 50 amino acid sequences for the M-polypeptide and 46 sequences of the L-polypeptide from a wide range of purple photosynthetic bacteria, constructed previously [49].

In order to facilitate binding of a BPhe rather than the more abundant BChl, it is necessary to ensure that the amino acid(s) positioned over the centre of the macrocycle cannot provide a fifth ligand to the central magnesium found in BChl. In the *Rb. sphaeroides* reaction centre, the relevant residues in the H_A binding pocket (Leu M214, Ala L124 and Phe L121) are suitably apolar. Introduction of a bonding histidine residue at the M214 or L124 position can cause replacement of the H_A BPhe by BChl (denoted β_A), showing that with appropriate modification this binding site is not specific to BPhe [32–34]. In the alignment a Leu was found at the M214 position except in 13 sequences that had Val, and three that had Ile. The L124 residue was Ala in 44 sequences and Pro in the remainder, whilst the L121 residue was absolutely conserved as Phe. As might be expected, therefore, this pocket is conserved for the binding of BPhe across the purple photosynthetic bacteria.

The equivalent amino acid residues adjacent to the centre of the H_B macrocycle the *Rb. sphaeroides* reaction centre are Leu L185, Ala M153 and Phe M150. Phe M150 was absolutely conserved and the M153 residue was Ala in all but one sequence, where it was Gly. The L185 residue showed more variety (Leu 38, Met 5, Phe 4, Trp 1, Ala 2), and it is possible that Met or Trp could provide a ligand to the magnesium of a BChl. However, a Trp is found at this position in *Rb. capsulatus*, which is known to contain a BPhe at the H_B position, and the sequences that contain Met at the L185 position included *Rhodopseudomonas viridis* (recently renamed *Blastochloris* (*Bcl.*) *viridis*), which is also known to contain a BPhe at the H_B position. Therefore, it seems likely that the H_B BPhe is also an absolutely conserved feature of those purple bacterial reaction centres where sequence information is available. One caveat to this is that an Ala side chain at the L185 position, as in two sequences for PufL from *Bcl. sulfoviridis* [49], could be sufficiently small to allow a ligating molecule such as water to be present in the binding pocket. As far as we are aware, the bacteriochlorin content of the *Bcl. sulfoviridis* reaction centre has not been described; a third deposited sequence for PufL from *Bcl. sulfoviridis* has a Met at the L185 position [49], as for the reaction centre from the closely related bacterium *Bcl. viridis*.

3.2. Replacement of the H_B BPhe with a BChl

To determine whether H_B could be replaced by a BChl, the symmetry-related residue to Leu M214 (see above), Leu L185, was mutated to His (mutant LL185H). The mutation was introduced as described in Materials and methods, and the mutant reaction centre genes were expressed to give strains with $RC^+LH1^-LH2^-$, $RC^+LH1^+LH2^-$ and $RC^+LH1^+LH2^+$ phenotypes. Examination of absorbance spectra of intact cells of the LL185H mutant in the $RC^+LH1^-LH2^-$ and $RC^+LH1^+LH2^-$ backgrounds indicated that the expression level of the LL185H reaction centre was normal. Fig. 2 compares the room temperature absorbance spectra of intracytoplasmic membranes from cells with a $RC^+LH1^+LH2^-$ phenotype containing wild-type or LL185H mutant reaction centres. The ratio of LH1 absorbance at 875 nm to reaction centre absorbance at 805 nm was similar in the two spectra, demonstrating that the level of reaction centre expression was not decreased by the LL185H mutation. Experiments with strains with an $RC^+LH1^+LH2^+$ phenotype (data not shown) showed that the LL185H mutation did not impair the capacity of the reaction centre to support
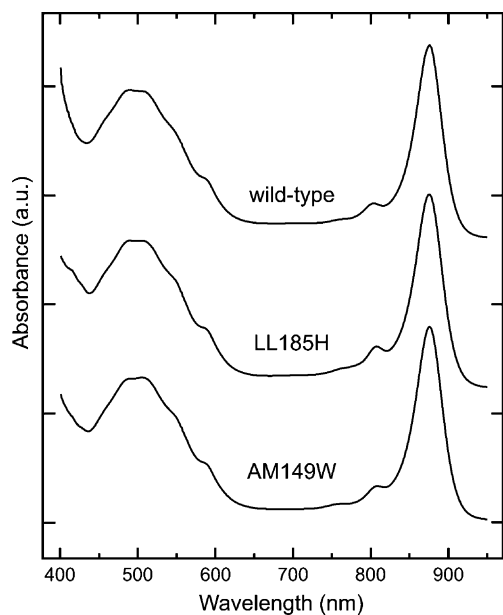
Fig. 2. Room temperature absorbance spectra of intracytoplasmic membranes from cells with a RC$^+$LH1$^+$LH2$^-$ phenotype. Spectra were normalised to approximately the same absorbance at 875 nm.

photosynthetic growth under the anaerobic/illuminated conditions described in a previous report [44].

Examination of the room temperature absorbance spectrum of intracytoplasmic membranes from strains with an RC$^+$LH1$^-$LH2$^-$ phenotype indicated that the LL185H mutation had affected the band at 756 nm (H Q$_y$ band) that is attributable to the two BPhes (data not shown). The band was flattened, and there was some indication of a new component in the spectrum around 778 nm. To examine this in more detail, spectra were recorded at 77 K (Fig. 3a). The 77 K spectrum of the membrane-bound wild-type reaction centre exhibited bands at 756 nm (H Q$_y$ band), 804 nm (attributed mainly to the monomeric BChls-B Q$_y$ band) and 893.5 nm (attributed to the P BChls-P Q$_y$ band). In the spectrum of the LL185H mutant the H Q$_y$ band was split into two components with maxima at 758.5 and 778.5 nm (Fig. 3a). This splitting was reminiscent of that reported previously for the LM214H mutant reaction centre (see above), the spectrum of which is shown for comparison in Fig. 3a. In good agreement with previous reports on detergent-purified reaction centres [32], the spectrum of the membrane-bound LM214H reaction centres showed two bands at 753 and 775 nm, which have previously been attributed to H$_B$ and β$_A$, respectively. An enlarged view of the H and B Q$_y$ bands in overlaid spectra is shown in Fig. 3b. The maximum of the B Q$_y$ band was unaffected in the spectrum of the LL185H mutant and was blue-shifted by 1 nm
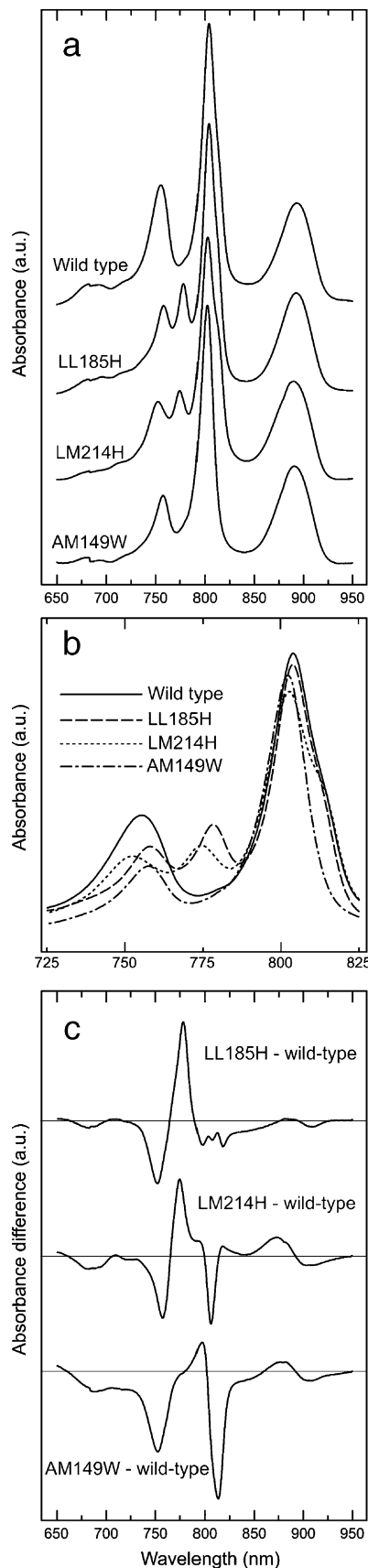
Fig. 3. (a) 77 K absorbance spectra of intracytoplasmic membranes from cells with a RC$^+$LH1$^-$LH2$^-$ phenotype. For the purposes of comparison, the spectra were corrected for background scatter (the region below 650 nm is not shown because of high background scatter from the membrane) and normalised to the same area of the P Q$_y$ band. Spectra are offset for comparison. (b) Overlaid spectra showing an enlarged view of the H and B Q$_y$ bands. (c) Mutant-minus-wild-type absorbance difference spectra calculated from the spectra in panel a.

in the spectrum of the LM214H mutant (Fig. 3b). The maximum of the P Q_y band was blue-shifted by 1 nm in the spectrum of the LL185H mutant and by 3.5 nm in the spectrum of the LM214H mutant (Fig. 3a).

The data in Fig. 3a and b provided good evidence that LL185H mutation had caused replacement of H_B by a BChl (denoted β_B). The new β_B absorbed at 778.5 nm, revealing the absorbance band of H_A at 758.5 nm. Taken together, the spectra of the LM214H and LL185H mutants showed clearly that H_A absorbs principally on the red side of the H Q_y band (at 758.5 nm at 77 K) whilst H_B absorbs principally on the blue side of this band (at 753 nm at 77 K) (Fig. 3b). In the wild-type a composite band is seen with a maximum at 756 nm at 77 K. It was interesting to note that β_A had an absorbance maximum 3.5 nm to the blue of β_B (Fig. 3b), and so the ordering of the bands was different for BChl and BPhe. The other point highlighted by the data in Fig. 3 is that, in both the LM214H and LL185H mutant, the intensity of the absorbance band of the new BChl was similar to that of the residual BPhe. This was also apparent in mutant-minus-wild-type difference spectra (Fig. 3c). In the case of the LM214H mutant this spectrum showed loss of a component at 757.5 nm together with appearance of a new component of similar intensity at 774.5 nm, whilst for the LL185H mutant the difference spectrum showed loss of a component at 752 nm together with appearance of a new component of similar intensity at 778.5 nm. The small blue-shift of the maximum of the B Q_y band caused by the LM214H mutation manifested in the difference spectrum as a sharp negative feature centred at 806 nm.

3.3. Exclusion of the H_B BPhe

Having established that H_B could be replaced with a BChl without affecting the expression level of the reaction centre, or its capacity to support photosynthetic growth, we next investigated whether the H_B cofactor could be removed altogether. The approach taken followed the lead provided by the AM260W mutation, that causes steric exclusion of the Q_A ubiquinone from the reaction centre [35,36]. Examination of a superimposition of the X-ray crystal structures of the wild-type and AM260W complexes showed that the M260 residue is located edge-on to the ring of the ubiquinone head-group, and that the Trp residue introduced at this position overlaps with, and is approximately coplanar to, this head-group [36]. Accordingly, the H_B binding pocket in the wild-type reaction centre was searched for small volume amino acid residues located edge-on to the BPhe ring, and consequently, residue Ala M149 was selected for mutation to Trp (AM149W).

The AM149W mutation was introduced and expressed as described in Materials and methods. Room temperature absorbance spectra for strains with $RC^+LH1^-LH2^-$ (not shown) and $RC^+LH1^+LH2^-$ phenotypes (Fig. 2) showed that the expression level of the AM149W reaction centre was normal. Examination of the room temperature spectrum of membranes from a strain with an $RC^+LH1^-LH2^-$ phenotype showed that the absorbance maximum of the B Q_y band was blue-shifted by approximately 4 nm relative to its position in

the spectrum of the wild-type complex, and the H Q_y band was reduced in amplitude, although the trough between the H and B Q_y bands was preserved (data not shown).

The 77-K absorbance spectrum of membrane-bound AM149W reaction centres is shown in Fig. 3a. The main effect of the AM149W mutation was a change in the absorbance maximum of the H Q_y band, from 756 nm in the spectrum of the wild-type to 758 nm in that of the AM149W mutant, and a reduction in the relative amplitude of this band. Unlike the spectra of the LL185H and LM214H mutants, the AM149W mutant gave only one band in the H Q_y region at 77 K. The absorbance maximum of the H Q_y band was almost identical (within 0.5 nm) to that of the shortest wavelength band in the 77 K spectrum of the LL185H mutant, which is assigned to H_A, and was similar in terms of area (Fig. 3b). The simplest interpretation of these effects was that the band at 758 nm in the spectrum of the AM149W mutant was attributable to H_A, and the absorbance of H_B normally centred at 753 nm was absent. A calculated AM149W-minus-wild-type difference spectrum (Fig. 3c) showed the loss of a component centred at 752.5 nm, very close to the absorbance maximum of the band attributed to H_B. Unlike the difference spectra for the LL185H and LM214H mutants also shown in Fig. 3c, the negative band at 752.5 nm in the difference spectrum of the AM149W mutant was not accompanied by a positive band of similar amplitude approximately 22–23 nm to the red, reinforcing the conclusion that the spectral change was due to the absence of the H_B BPhe, rather than replacement of BPhe by BChl.

In addition to this change, the maximum of the B Q_y band of the AM149W reaction centre was approximately 2 nm to the blue of that seen for the wild-type complex, and the band was noticeably sharper, with a loss of the shoulder that is visible on the red side of the B Q_y band in the wild-type reaction centre (and is better resolved in the LM214H mutant) (Fig. 3b). This suggested an additional effect of the AM149W mutation on the absorbance properties of B_B, probably a shift of the Q_y band of B_B to higher energies, which would be expected to cause the composite B Q_y band to blue-shift and become more symmetrical. The calculated AM149W-minus-wild type difference spectrum showed a shift of a component from 813.5 nm to 797 nm (Fig. 3c), consistent with this.

3.4. Crystallographic analysis of the AM149W mutant

Taken together with the spectra of the LL185H and LM214H mutants, the 77 K spectrum of the AM149W mutant strongly suggested that the Ala to Trp mutation had caused the reaction centre to assemble without H_B. To look directly at the structural changes caused by this mutation, the AM149W reaction centre was purified as described in Materials and methods, with a view to crystallising the complex. Solubilisation of the AM149W reaction centre from antenna-deficient membranes using 1.5% LDAO was followed by a standard purification procedure employing three ion exchange columns and a gel filtration column. During this procedure, it was noticeable that the AM149W reaction centre was somewhat

unstable, showing a greater than normal tendency to degrade with the appearance of free BChl in column eluates. However, despite this it was possible to purify sufficient quantities of the AM149W mutant for crystallisation.

To examine whether purification had produced any further changes in the bacteriochlorin content of the AM149W reaction centre, the 77-K absorbance spectra of purified AM149W and wild-type reaction centres were recorded and compared (Fig. 4a). The absorbance changes in the Q_y region seen for the membrane-bound AM149W reaction centre (Fig. 3) were similar to those seen for the purified complex (Fig. 4a). These were a decrease in relative intensity and 3 nm red-shift of the H Q_y band, a 2-nm blue-shift, sharpening and increase in relative intensity of the B Q_y band and a 7-nm blue-shift of the P Q_y band, which also had broadened somewhat. In addition, the band at 534 nm in the spectrum of the wild-type reaction centre (Fig. 4a, arrow), attributed to the Q_x transition of H_B [50,51], was absent from the spectrum of the AM149W complex. This provided further evidence for the absence of H_B in this mutant reaction centre. The Q_x band of the H_A BPhe at 545 nm was unaffected (Fig. 4a). The absorbance maximum of the asymmetric band at 598 nm in the spectrum of the wild-type reaction centre, attributed to all four reaction centre BChls, was blue-shifted by 1–2 nm in the spectrum of the AM149W mutant. Fig. 4b also shows a calculated AM149W-minus-wild-type difference spectrum, which highlights loss of the H_B Q_x and Q_y bands (troughs at 533 and 755 nm), and a shift of part of the B Q_y band from 813.5 to 797 nm. The latter feature is consistent with a change in the properties of the B_B BChl,

shifting the Q_y transition of this BChl from its expected position at around 814 nm [51–53] to higher energies, and this result matched findings with membrane-bound reaction centres (Fig. 3c). The reaction centre carotenoid gives rise to relatively low intensity absorbance bands between 400 and 550 nm, and there were no obvious changes in spectrum in this region that could be ascribed to a change in the spectrum of the reaction centre carotenoids caused by the AM149W mutation.

The AM149W reaction centre was crystallised in a trigonal form as described in Materials and methods, and diffraction data was collected using cryo-cooled crystals and an ADSC Quantum 4 detector, on beam-line 14.1 of the Daresbury Synchrotron Facility, U.K. Reflecting the limited quality of the available crystals, the dataset collected for the AM149W mutant was at a rather modest resolution (3.4 Å) and completeness (Table 1). Given this the structure was only partially refined, focussing on the area around the H_B site and the adjacent B-branch cofactors. As a result the partially refined structure had rather high R factors (R-factor=24.7%, R_{free}=29.2%) and these data can only be described as preliminary findings. Nevertheless, despite these limitations the electron density map was sufficiently clear to allow the conclusion that the mutation had not caused any significant changes in the overall structure of the reaction centre (e.g., the conformation of the polypeptide backbone and positions of the other cofactors). However, there was evidence of a significant change in the region adjacent to the mutated M149 residue, in addition to extra density at the M149 position due to the Ala to Trp change. Modelling of this area was carried out on the basis of omit maps, with the H_B BPhe absent in the initial round of refinement.

Fig. 5a is a view of the H_B pocket and the M149 residue in an mF_o-DF_c difference map calculated with the M149 residue retained as Ala and including the H_B BPhe. The map showed positive density adjacent to the M149 residue, and negative density for much of the BPhe macrocycle and side-chain (rings I–V of the BPhe macrocycle are labelled in Fig. 5a). These data were consistent with replacement of the M149 Ala by a larger residue, and the conclusion from the spectroscopic data that the H_B BPhe was absent. Fig. 5b shows the $2mF_o-DF_c$ electron density map and final fitted structure for this region of the protein. The H_B BPhe from the wild-type reaction centre is overlaid (thin stick model, cyan carbon atoms). As can be seen, the electron density for the new Trp at the M149 position was resolved, and the modelled Trp was orientated approximately co-planar with the BPhe macrocycle, overlapping space normally occupied by ring III of the H_B macrocycle.

Two regions of density were observed in the H_B binding pocket, labelled A and B in Fig. 5b, the origins of which were unclear. One was an elongated electron density feature in the region normally occupied by rings I, II and IV of the BPhe macrocycle (B in Fig. 5b), whilst the other was near ring V (A in Fig. 5b). The limited resolution made it impossible to assign either feature with any degree of certainty, but they could arise from detergents, lipids, the side chains of neighbouring cofactors or other components of the crystallisation mix such as heptanetriol. Turning to the remainder of the binding pocket,
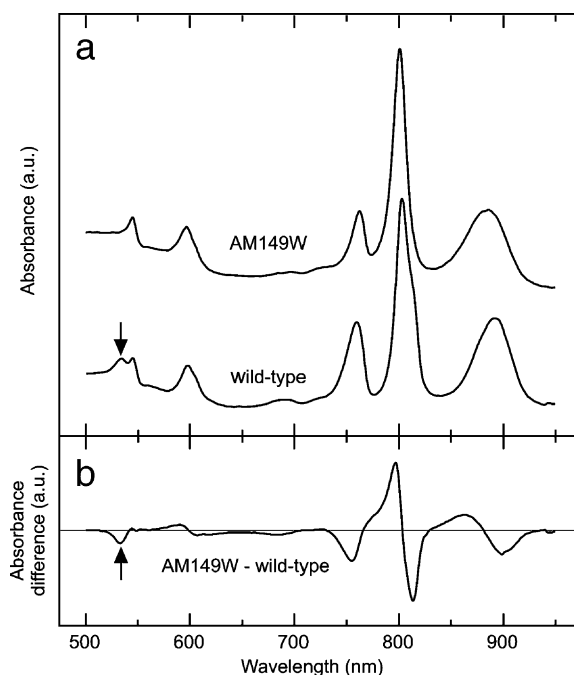

Fig. 4. (a) 77 K absorbance spectra of purified reaction centres. Spectra were normalised to approximately the same area of the P Q_y band, and are offset for comparison. (b) Mutant-minus-wild-type absorbance difference spectra calculated from the spectra in panel a. The arrows in panels a and b indicate the position of the Q_X absorbance band of H_B in the spectrum of the wild-type reaction centre.
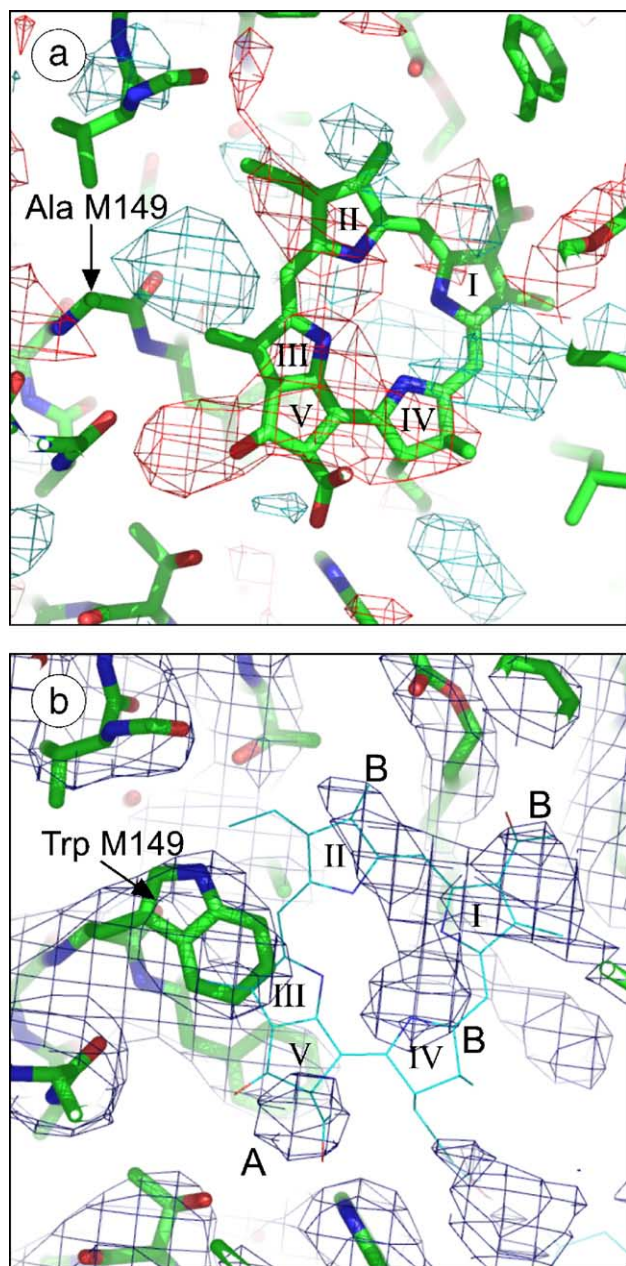
Fig. 5. Electron density maps for the region around the M149 residue and H_B BPhe in the AM149W reaction centre. (a) $mF_o - DF_c$ difference density map, contoured at 3σ, calculated with Ala at the M149 position and a BPhe present at the H_B position, with rings I–V labelled. Positive density is in cyan, negative density in red. The structural model of the AM149W reaction centre is shown in cpk colours except for carbons which are in green. The methyl side chain of Ala M149 projects outwards from the plane of the page, and is indicated by the arrow. (b) $2mF_o - DF_c$ electron density map and fitted structure for the AM149W reaction centre. The position of the H_B BPhe in the wild-type reaction centres is overlaid (thin stick model, cpk colours but cyan carbons) and rings I–V are indicated. Labels A and B indicate electron density features of uncertain origin (see text).

there did not appear to be any large scale repositioning of amino acid side chains in response to the loss of H_B, or deviations in the position of the polypeptide backbones. As a result, apart from the two unassigned electron density features and the extra density due to the enlarged M149 side-chain, the remainder of the pocket was empty, and there was no

significant collapse of the structure of the surrounding protein in response to the loss of H_B. The limited resolution of the data precluded an analysis of detailed changes in the structure of the H_B binding pocket.

3.5. Functional effects of the AM149W mutation

The data described above demonstrated that the reaction centre can assemble in the membrane in the absence of a cofactor at the H_B site. Possible functional consequences of the loss of this cofactor were examined in three ways. First, the ability of the AM149W reaction centre to support photosynthetic growth of *Rb. sphaeroides* was assessed, and it was found that the mutation had no discernable effect on the ability of the bacterium to grow under anaerobic illuminated conditions (data not shown). This implied that energy transfer into the reaction centre, A-branch electron transfer and Q_B site function must still be operational in the AM149W reaction centre (although this assay would not necessarily pick up any non-lethal impairments of these processes if they were not rate-limiting for growth).

Second, FTIR difference spectroscopy was used to look at the end product of light-induced electron transfer in the reaction centre, the radical Q_B^-. These experiments were performed on purified reaction centres in which Q_B had been reconstituted with a ten-fold molar excess of Q_3, as described in Materials and methods. Fig. 6 compares the FTIR difference spectra obtained at 290 K with wild-type (Fig. 6a) and AM149W (Fig. 6b) reaction centres. These spectra were generated under low-intensity continuous illumination. However, highly comparable Q_B^-/Q_B spectra were also obtained under single turnover flash excitation (data not shown). The Q_B^-/Q_B difference spectrum obtained with wild-type reaction centres was identical to that obtained previously for *Rb. sphaeroides* wild-type and R26 reaction centres [40–42,54]. The spectrum of the AM149W reaction centre had a similar
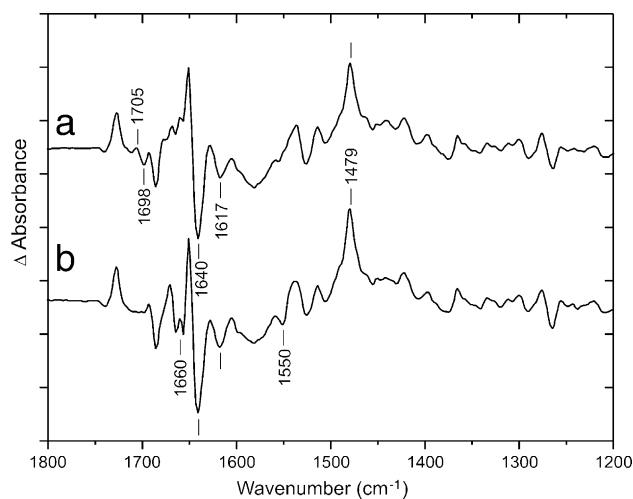

Fig. 6. Light-induced $P^+Q_B^-/PQ_B$ FTIR difference spectra at 285 K of (a) wild-type and (b) AM149W reaction centres reconstituted with Q_3. Tick marks on the vertical axis are separated by 10^{-4} absorbance units. Spectral resolution is 4 cm^{-1}.

lineshape and showed characteristic bands of the disappearing Q_B state (negative bands at 1685, 1640, 1617, 1527, 1290 and 1265 cm^{-1}) and appearing Q_B^- state (positive bands at 1728, 1651, 1537, 1514, 1479 and 1365 cm^{-1}) [40–42,54].

The principal difference found was the absence from the spectrum of the AM149W mutant of a differential signal at 1705/1698 cm^{-1} (indicated on the spectrum of wild-type in Fig. 6a). This differential signal observed in the wild type reaction centre is found in the infrared frequency range characteristic of the 9-keto carbonyl of H_B as previously reported from resonance Raman experiments [55–58]. The absence of this differential signal in the spectrum of the AM149W reaction centre (Fig. 6b) was therefore consistent with an assignment of this signal in the wild-type reaction centre to an electrostatic influence of Q_B^- on the vibrational mode of the 9-keto carbonyl of H_B. A comparable electrostatic influence of Q_A^- on infrared carbonyl modes of H_A has previously been described in reaction centers of both *Rb. sphaeroides* [59] and *Bcl. viridis* [60]. In addition, small differences in the regions around 1660 and 1550 cm^{-1} were observed between the spectra of the wild-type and mutant reaction centre. The bands affected were in the amide I (at 1660 cm^{-1}) and amide II (at 1550 cm^{-1}) absorption ranges [61], and the differences probably reflected small variations in the relaxation of the protein upon Q_B^- formation in the AM149W mutant compared to the wild-type reaction centre.

The FTIR data showed that the state Q_B^- was formed in the AM149W reaction centre in response to photoexcitation, and there were no strong perturbations of the Q_B^-/Q_B spectrum that might indicate disruption of the Q_B site. This was in general agreement with the results of X-ray crystallography (see above), which gave no indication of large scale structural changes affecting the Q_B site. The binding position of the Q_B ubiquinone was not clear from the crystallographic data, because the quality of the maps in this region was insufficient to allow modelling of the ubiquinone head-group with any

degree of certainty (data not shown). However, the identical frequency of the bands assigned to the main vibrational modes of Q_B (at 1640 and 1617 cm^{-1}) and Q_B^- (at 1479 cm^{-1}) for both the wild-type and AM149W reaction centre (Fig. 6b) provides evidence that the quinone was localised at the so-called proximal Q_B site in the AM149W mutant [40,54,62].

Finally, femtosecond time-scale transient absorbance spectroscopy was used to examine the effects of H_B replacement or exclusion on the characteristics of A-branch electron transfer, as described in Materials and methods. Absorbance difference spectra were recorded over the wavelength range 700–950 nm at varying time intervals up to 3–4 ns, using a 60 fs excitation pulse centred at 795 nm (data not shown). Samples consisted of intracytoplasmic membranes from strains with RC$^+$LH1$^-$LH2$^-$ phenotype containing wild-type, LL185H or AM149W reaction centres. Data was analysed globally using a linear sequential model (i.e. 1→2→3→). In all three cases four temporally and spectrally-distinct states were required to describe the data (Fig. 7), attributed to the states B*, P*, P$^+$H$_A^-$ and P$^+$Q$_A^-$ as reported in previous publications [44,63–66]. The state B* is a mixture of B$_B$* and (mainly) B$_A$* formed by the 795 nm excitation pulse [44,66]. The lifetimes of the P* and P$^+$H$_A^-$ states in the membrane-bound wild-type complex, 5 ps and 200 ps [44,63,64], were not altered in the two mutant complexes. In all three reaction centres the final state was P$^+$Q$_A^-$; this spectrum is absent in reaction centres that lack the Q$_A$ ubiquinone [65]. The lifetime of the B* state formed by the 795 nm excitation pulse was 150 fs for the wild-type, 160 fs for the AM149W mutant and 220 fs for the LL185H mutant. Although these differences were small, the slightly longer lifetime for the LL185H mutant could reflect the fact that this complex has three monomeric BChls absorbing in the 800 nm region, with the new β$_B$ absorbing on the blue side of the B Q$_y$ band. As a result the 795 nm excitation pulse could have excited some β$_B$, producing the additional energy transfer
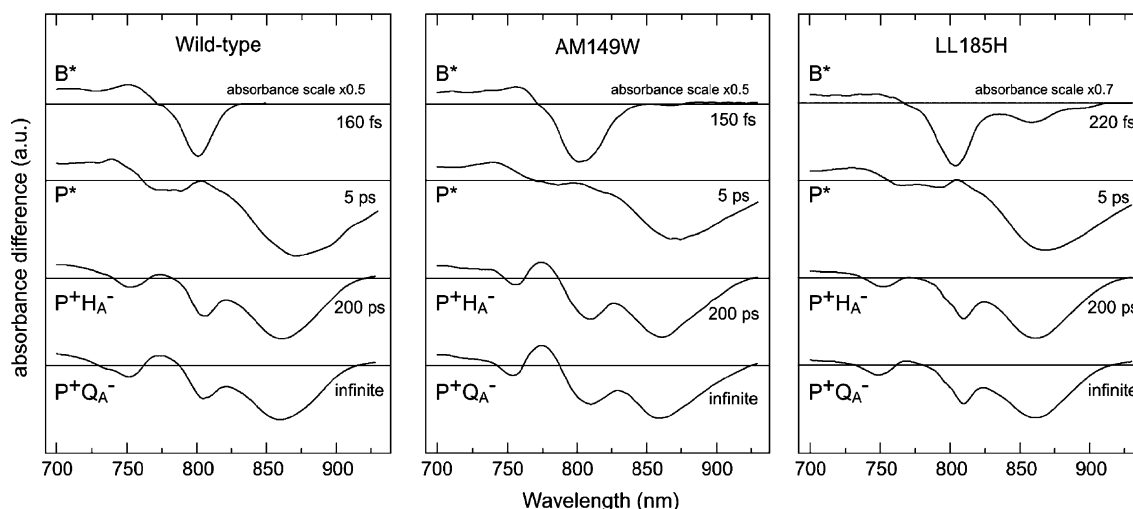

Fig. 7. SADS and associated lifetimes derived from a global analysis of transient absorbance spectra obtained after 795 nm excitation. The state attributed to each species is indicated. For the purposes of comparison, spectra attributed to the state B* were multiplied by factors of 0.5 (wild-type), 0.5 (AM149W) and 0.7 (LL185H).

step $\beta_B^* \rightarrow B_B^*$ and extending the lifetime of the mixed species B*. This aside, neither mutation had a measurable effect on the rate of primary or secondary charge separation.

4. Discussion

The combination of spectroscopic and crystallographic data presented above showed that mutation of Leu L185 to His caused the *Rb. sphaeroides* reaction centre to assemble with a BChl at the H_B position, whilst mutation of Ala M149 to Trp caused the complex to assemble without either BPhe or BChl at the H_B site. Although the resolution of crystallographic data on the latter mutant precluded a detailed description of the structural effects of exclusion of the H_B cofactor, it was possible to conclude that there were no major changes in the structure of the remainder of the protein-cofactor system. This correlated with unchanged time constants for A-branch charge separation and good evidence from FTIR spectroscopy that the adjacent Q_B site was largely unperturbed. 77 K absorbance spectroscopy showed that the properties of the B_B BChl were sensitive to loss of the adjacent cofactor, with a shift of the Q_y absorbance band of B_B to 797 nm from 813.5 nm (Figs. 3c and 4b). The position of this band in the absolute spectrum of the wild-type reaction centre is not particularly well resolved due to overlap with the Q_y absorbance band of B_A, but it is more visible in the spectrum of the LM214H mutant due to a blue-shift of the B_A absorbance band (Fig. 3b).

The AM149W and LL185H mutations provide opportunities for investigating the possible function of the BPhe at the H_B site. As outlined in the Introduction two questions arise concerning this cofactor, namely why has the H_B cofactor been retained in purple bacteria (and indeed in all Type II reaction centres), and why is this cofactor preserved as a BPhe rather than the more common BChl? It does not seem to be required for light-driven charge separation or ubiquinol production, and has not been assigned a role in photoprotection by the carotenoid cofactor. One possible answer that can now be discounted is that the H_B cofactor is required for the proper assembly or structural stability of the complex, as H_B can be excluded from the reaction centre with little effect on the structure of the remainder of the complex. The expression level of the H_B-deficient reaction centre was normal (unstable mutants often show lowered levels of expression in the membrane relative to the LH1 antenna), and the bacterium was still capable of photosynthetic growth. It was the case that the AM149W reaction centre was somewhat less stable than the wild-type on removal from the membrane, but this is probably of little functional or physiological significance. In particular, the structural and functional integrity of the Q_B site was preserved in the absence of H_B, and so we can exclude the possibility that H_B is required to provide structural support for the adjacent Q_B pocket. One possibility that remains is that the H_B cofactor is required to provide structural stability to the membrane-bound reaction centre under conditions of stress that have not been addressed in the experiments described above. It has been established that photosynthetic growth is possible in the absence of the H_B cofactor under benign conditions

(optimal growth temperature, absence of oxygen and high light intensities), but it could be that the reaction centre would be compromised by the AM149W mutation during growth under more stressful conditions, such as elevated temperature for example.

If the reaction centre is capable of assembling in a functional form in the absence of the H_B cofactor, what other role could this BPhe be playing? One obvious function is as an accessory light harvesting pigment [14,15]. Retention of a BPhe at the H_B position would ensure downhill energy transfer to P via B_B. However, in wild-type strains the reaction centre is surrounded by a large number of light harvesting BChls and carotenoids, and the relative importance of a single 760 nm-absorbing cofactor seems questionable.

Woodbury and co-workers have proposed that H_B participates in photoprotection of the reaction centre following absorption of photons in the blue/UV regions of the spectrum [30]. The proposal stems from the observation that excitation of the *Rb. sphaeroides* reaction centre at 390 nm results in the formation, within a few hundred femtoseconds, of a radical pair state assigned as $B_B^+ H_B^-$. In purified reaction centres lacking Q_B this state has a lifetime of approximately 15 ps at room temperature, and over 1 ns at 10 K [30]. It is proposed that ultrafast formation of radical pairs on the B-branch could provide a mechanism to dissipate the energy of high-energy excited states formed by blue light excitation of the bacteriochlorin pigments, or UV excitation of the tryptophan residues of the protein [30]. The physiological significance of such a photoprotective mechanism remains to established, but if it is of relevance then this could explain why a BPhe cofactor has been retained at the H_B position, as a $B_B^+ \beta_B^-$ state would be expected to have different properties to the $B_B^+ H_B^-$ state proposed to be formed by 390 nm excitation. The data outlined above show that photosynthetic growth per se is not prevented by replacement or removal of the H_B BPhe, but the mutant complexes described in this report would provide a system for examining whether photosynthetic growth under particular stress conditions is affected by changes to the B-branch cofactors.

Perhaps, the most obvious function of the H_B BPhe is to make the B-branch complete, such that any electrons that take the "wrong" route during primary charge separation can nevertheless be transferred to the Q_B site, maximising the efficiency of energy transduction. By analogy with the A-branch, a BPhe cofactor at the H_B site would provide a free energy drop for the transition $P^+ B_B^-$ to $P^+ H_B^-$ that would contribute to the efficiency of electron transfer along the B-branch. Having said this, a number of estimates of the relative activities of the A- and B-branch have been made [29,33,67], and these suggest that the B-branch plays an insignificant role in the catalysis of transmembrane electron transfer. This would call into question the necessity to have an intact and efficiently functioning B-branch, unless the relative flux of electrons along the B-branch is larger in reaction centres in intact, native membranes than estimates made on purified reaction centres would seem to indicate.

Another problem concerns the rates of individual electron transfer steps along the B-branch. The B-branch reaction

$P* \rightarrow P^+H_B^-$ has been estimated to occur with a lifetime of around 200 ps in *Rb. sphaeroides*, as compared with $\sim$3 ps for the equivalent A-branch $P* \rightarrow P^+H_A^-$ reaction [50]. Similarly, recent estimates indicate that the reaction $P^+H_B^- \rightarrow P^+Q_B^-$ is at least a factor of 10 slower than the corresponding A-branch reaction, with a rate estimated in the range $2–12$ ns^{-1} compared with $\sim$200 ps^{-1} for $P^+H_A^- \rightarrow P^+Q_A^-$ [68–70]. As the rate of $P^+H_B^-$ decay by charge recombination is estimated to be $1–4$ ns^{-1} [69], this implies that the electron transfer step from H_B^- to Q_B will be less than 100% efficient due to competition from charge recombination. Although this may be an inescapable consequence of the different characters of the Q_A and Q_B sites, imposed by their different roles, it would be curious if an intact B-branch of cofactors has been retained in order to ensure that any electrons that proceed along this branch can be delivered to Q_B, maximising quantum yield, but this is undermined by having an inefficient electron transfer step from H_B^- to Q_B.

Finally, a point relevant to the question of the role of the H_B BPhe in the purple bacterial reaction centre is the fact that a pheophytin is also conserved at this position in Photosystem II (PS-II). This could mean that the role of the H_B cofactor is common to both types of reaction centre, despite the evolutionary gap between them. However, Xiong and co-workers have recently described the properties of a PS-II reaction centre from *Chlamydomonas reinhardtii* in which the inactive branch pheophytin is replaced by a chlorophyll, through mutation of residue Leu 210 of the D1 polypeptide to His [71]. The mutation did not affect the assembly of PS-II, and mutant PS-II reaction centres could be prepared using standard protocols. However, the altered PS-II complex showed a serious impairment of A-branch charge separation, with a very limited capacity for reduction of Q_A or oxygen evolution [71]. The mutant reaction centres also showed larger amounts of chlorophyll fluorescence, and the effects of the pheophytin to chlorophyll mutation were interpreted as indicating a change in the distribution of excited state energy amongst the six chlorin cofactors of the reaction centre, excitation energy being focussed on the B-branch pigments producing a drastically reduced level of A-branch charge separation [71]. These findings are clearly very different to those for the LL185H mutant described above, and indicate that conservation of a pheophytin cofactor at the H_B position in PS-II may be necessary for completely separate reasons to those governing conservation of a BPhe at this position in the purple bacterial reaction centre.

4.1. Summary

The functional basis for conservation of a BPhe cofactor at the H_B site in the purple bacterial reaction centre remains undecided. However, as a result of the findings described in this report, it can be ruled out that this BPhe is required for assembly of the reaction centre, the structural or functional integrity of the adjacent Q_B site, optimal operation of light driven charge separation along the A-branch of cofactors, or photosynthetic growth of the organism. It is possible that this BPhe cofactor is required in order to complete the B-branch of cofactors, for reasons relating to transmembrane electron transfer that are not yet clear. Alternatively, it may participate in photoprotective charge separation reactions involving other B-branch cofactors, act as a light harvesting pigment, or be required to stabilise the reaction centre protein under conditions of stress. However, the physiological relevance of each of these possibilities remains to be established. Recent findings on the PS-II reaction centre indicate a markedly different sensitivity to replacement of the H_B cofactor with a chlorophyll, probably arising from differences in the energy coupling between the six (bacterio)chlorin cofactors in the two types of reaction centre. In PS-II, a pheophytin cofactor is needed at the H_B position in order to preserve core function, whereas in purple bacteria the core function of the reaction centre is essentially unaffected even if the H_B cofactor is completely absent from the complex.

Acknowledgements

References

[1] J.P. Allen, G. Feher, T.O. Yeates, H. Komiya, D.C. Rees, Structure of the reaction center from *Rhodobacter sphaeroides* R-26: the cofactors, Proc. Natl. Acad. Sci. U. S. A. 84 (1987) 5730–5734.

[2] J.P. Allen, G. Feher, T.O. Yeates, H. Komiya, D.C. Rees, Structure of the reaction center from *Rhodobacter sphaeroides* R-26: the protein subunits, Proc. Natl. Acad. Sci. U. S. A. 84 (1987) 6162–6166.

[3] C.H. Chang, O. El Kabbani, D. Tiede, J. Norris, M. Schiffer, Structure of the membrane-bound protein photosynthetic reaction center from *Rhodobacter sphaeroides*, Biochemistry 30 (1991) 5352–5360.

[4] U. Ermler, G. Fritzsch, S.K. Buchanan, H. Michel, Structure of the photosynthetic reaction centre from *Rhodobacter sphaeroides* at 2.65-angstrom resolution: cofactors and protein–cofactor interactions, Structure 2 (1994) 925–936.

[5] U. Ermler, H. Michel, M. Schiffer, Structure and function of the photosynthetic reaction center from *Rhodobacter sphaeroides*, J. Bioenerg. Biomemb. 26 (1994) 5–15.

[6] W.W. Parson, Reaction centers, in: H. Scheer (Ed.), Chlorophylls, CRC Press, Boca Raton, FL, USA, 1991, pp. 1153–1180.

[7] N.W. Woodbury, J.P. Allen, The pathway, kinetics and thermodynamics of electron transfer in wild type and mutant bacterial reaction centers of purple nonsulfur bacteria, in: R.E. Blankenship, M.T. Madigan, C.E. Bauer (Eds.), Anoxygenic Photosynthetic Bacteria, Kluwer Academic Publishers, The Netherlands, 1995, pp. 527–557.

[8] W.W. Parson, Photosynthetic bacterial reaction centers, in: D.S. Bendall (Ed.), Protein Electron Transfer, BIOS Scientific Publishers, Oxford, UK, 1996, pp. 125–160.

[9] A.J. Hoff, J. Deisenhofer, Photophysics of photosynthesis: structure and spectroscopy of reaction centres of purple bacteria, Phys. Rep. 287 (1997) 2–247.

[10] M.E. Van Brederode, M.R. Jones, Reaction centres of purple bacteria, in: N.S. Scrutton, A. Holzenburg (Eds.), Enzyme-Catalysed Electron and Radical Transfer, Kluwer Academic/Plenum Publishers, New York, USA, 2000, pp. 621–676.

[11] M.Y. Okamura, M.L. Paddock, M.S. Graige, G. Feher, Proton and electron transfer in bacterial reaction centers, Biochim. Biophys. Acta 1458 (2000) 148–163.

[12] C.A. Wraight, Proton and electron transfer in the acceptor quinone complex of photosynthetic reaction centers from *Rhodobacter sphaeroides*, Front. Biosci. 9 (2004) 309–337.

[13] H.A. Frank, Carotenoids in photosynthetic bacterial reaction centers: structure, spectroscopy and photochemistry, in: J. Deisenhofer, J.R. Norris (Eds.), The Photosynthetic Reaction Center, vol. 2, Academic Press, San Diego, USA, 1993, pp. 221–239.

[14] R.J. Cogdell, W.W. Parson, M. Kerr, The type, amount, location, and energy transfer properties of the carotenoid in reaction centers from *Rhodopseudomonas sphaeroides*, Biochim. Biophys. Acta 430 (1976) 83–93.

[15] S. Lin, E. Katilius, A.K.W. Taguchi, N.W. Woodbury, Excitation energy transfer from carotenoids to bacteriochlorophyll in the photosynthetic purple bacterial reaction centre of *Rhodobacter sphaeroides*, J. Phys. Chem., B 107 (2003) 14103–14108.

[16] H.A. Frank, R.J. Cogdell, Carotenoids in photosynthesis, Photochem. Photobiol. 63 (1996) 257–264.

[17] R.J. Cogdell, T.D. Howard, R. Bittl, E. Schlodder, I. Geisenheimer, W. Lubitz, How carotenoids protect bacterial photosynthesis, Philos. Trans. R. Soc. London B 355 (2000) 1345–1349.

[18] A. Angerhofer, V. Aust, A monomeric bacteriochlorophyll triplet state (^{3}B) in reaction centers of *Rhodobacter sphaeroides* R26, studied by absorption detected magnetic resonance, Photochem. Photobiol., B 20 (1993) 127–132.

[19] H.A. Frank, V. Chynwat, G. Hartwich, M. Meyer, I. Katheder, H. Scheer, Carotenoid triplet state formation in *Rhodobacter sphaeroides* R-26 reaction centers exchanged with modified bacteriochlorophyll pigments and reconstituted with spheroidene, Photosynth. Res. 37 (1993) 193–203.

[20] G. Hartwich, H. Scheer, V. Aust, A. Angerhofer, Absorption and ADMR studies on bacterial photosynthetic reaction centres with modified pigments, Biochim. Biophys. Acta 1230 (1995) 97–113.

[21] H.A. Frank, V. Chynwat, A. Posteraro, G. Hartwich, I. Simonin, H. Scheer, Triplet state energy transfer between the primary donor and the carotenoid in *Rhodobacter sphaeroides* R-26.1 reaction centers exchanged with modified bacteriochlorophyll pigments and reconstituted with spheroidene, Photochem. Photobiol. 64 (1996) 823–831.

[22] P.D. Laible, V. Chynwat, M.C. Thurnauer, M. Schiffer, D.K. Hanson, H.A. Frank, Protein modifications affecting triplet energy transfer in bacterial photosynthetic reaction centers, Biophys. J. 74 (1998) 2623–2637.

[23] A. Angerhofer, V.A. Bornhauser, V. Aust, G. Hartwich, H. Scheer, Triplet energy transfer in bacterial photosynthetic reaction centers, Biochim. Biophys. Acta 1365 (1998) 404–420.

[24] A. deWinter, S.G. Boxer, The mechanism of triplet energy transfer from the special pair to the carotenoid in bacterial photosynthetic reaction centers, J. Phys. Chem. 103 (1999) 8786–8789.

[25] P.D. Laible, Z.S. Morris, M.C. Thurnauer, M. Schiffer, D.K. Hanson, Inter- and intraspecific variation in excited-state triplet energy transfer rates in reaction centers of photosynthetic bacteria, Photochem. Photobiol. 78 (2003) 114–123.

[26] Z.S. Morris, D.K. Hanson, P.R. Pokkuluri, D.G. Mets, A.N. Hata, O.G. Poluektov, M.C. Thurnauer, M. Schiffer, P.D. Laible, Lysine substitutions near photoactive cofactors in the bacterial photosynthetic reaction center have opposite effects on the rate of triplet energy transfer, Chem. Phys. 294 (2003) 329–346.

[27] J.B. Arellano, T.B. Melo, P.K. Fyfe, R.J. Cogdell, K.R. Naqvi, Multichannel flash spectroscopy of the reaction centers of wild-type and mutant *Rhodobacter sphaeroides*: Bacteriochlorophyll$_B$-mediated interaction between the carotenoid triplet and the special pair, Photochem. Photobiol. 79 (2004) 68–75.

[28] H.A. Frank, C.A. Violette, Monomeric bacteriochlorophyll is required for the triplet energy-transfer between the primary donor and the carotenoid in photosynthetic bacterial reaction centers, Biochim. Biophys. Acta 976 (1989) 222–232.

[29] R.E. Blankenship, Molecular Mechanisms of Photosynthesis, Blackwell Science Ltd., Oxford, UK, 2002, pp. 100–102.

[30] S. Lin, E. Katilius, A.L.M. Haffa, A.K.W. Taguchi, N.W. Woodbury, Blue light drives B-side electron transfer in bacterial photosynthetic reaction centers, Biochemistry 40 (2001) 13767–13773.

[31] A.L.M. Haffa, S. Lin, J.C. Williams, B.P. Bowen, A.K.W. Taguchi, J.P. Allen, N.W. Woodbury, Controlling the pathway of photosynthetic charge separation in bacterial reaction centers, J. Phys. Chem. 108 (2004) 4–7.

[32] C. Kirmaier, D. Gaul, R. Debey, D. Holten, C.C. Schenck, Charge separation in a reaction center incorporating bacteriochlorophyll for photoactive bacteriopheophytin, Science 251 (1991) 922–927.

[33] B.A. Heller, D. Holten, C. Kirmaier, Control of electron-transfer between the L-side and M-side of photosynthetic reaction centers, Science 269 (1995) 940–945.

[34] B.A. Heller, D. Holten, C. Kirmaier, Characterization of bacterial reaction centers having mutations of aromatic residues in the binding-site of the bacteriopheophytin intermediary electron carrier, Biochemistry 34 (1995) 5294–5302.

[35] J.P. Ridge, M.E. van Brederode, M.G. Goodwin, R. van Grondelle, M.R. Jones, Mutations that modify or exclude binding of the Q_A ubiquinone and carotenoid in the reaction center from *Rhodobacter sphaeroides*, Photosynth. Res. 59 (1999) 9–26.

[36] K.E. McAuley, P.K. Fyfe, J.P. Ridge, R.J. Cogdell, N.W. Isaacs, M.R. Jones, Ubiquinone binding, ubiquinone exclusion, and detailed cofactor conformation in a mutant bacterial reaction center, Biochemistry 39 (2000) 15032–15043.

[37] K.E. McAuley-Hecht, P.K. Fyfe, J.P. Ridge, S.M. Prince, C.N. Hunter, N.W. Isaacs, R.J. Cogdell, M.R. Jones, Structural studies of wild type and mutant reaction centers from an antenna-deficient strain of *Rhodobacter sphaeroides*: monitoring the optical properties of the complex from cell to crystal, Biochemistry 37 (1998) 4740–4750.

[38] M.R. Jones, G.J.S. Fowler, L.C.D. Gibson, G.G. Grief, J.D. Olsen, W. Crielaard, C.N. Hunter, Construction of mutants of *Rhodobacter sphaeroides* lacking one or more pigment–protein complexes and complementation with reaction-centre, LH1, and LH2 genes, Mol. Microbiol. 6 (1992) 1173–1184.

[39] M.R. Jones, M. Heer-Dawson, T.A. Mattioli, C.N. Hunter, B. Robert, Site-specific mutagenesis of the reaction centre from *Rhodobacter sphaeroides* studied by Fourier transform Raman spectroscopy: mutations at tyrosine M210 do not affect the electronic structure of the primary donor, FEBS Lett. 339 (1994) 18–24.

[40] J. Breton, C. Boullais, G. Berger, C. Mioskowski, E. Nabedryk, Binding-sites of quinones in photosynthetic bacterial reaction centers investigated by light-induced FTIR difference spectroscopy: symmetry of the carbonyl interactions and close equivalence of the Q_B vibrations in *Rhodobacter sphaeroides* and *Rhodopseudomonas viridis* probed by isotope labeling, Biochemistry 34 (1995) 11606–11616.

[41] E. Nabedryk, J. Breton, R. Hienerwadel, C. Fogel, W. Mäntele, M.L. Paddock, M.Y. Okamura, Fourier transform infrared difference spectroscopy of secondary quinone acceptor photoreduction in proton transfer mutants of *Rhodobacter sphaeroides*, Biochemistry 34 (1995) 14722–14732.

[42] J. Breton, C. Berthomieu, D.L. Thibodeau, E. Nabedryk, Probing the secondary quinone (Q_B) environment in photosynthetic bacterial reaction centers by light-induced FTIR difference spectroscopy, FEBS Lett. 288 (1991) 109–113.

[43] C.C. Gradinaru, I.H.M. van Stokkum, A.A. Pascal, R. van Grondelle, H. van Amerongen, Identifying the pathways of energy transfer between carotenoids and Chlorophylls in LHCII 30.and CP29: a multicolor, femtosecond pump-probe study, J. Phys. Chem., B 104 (2000) 9330–9342.

[44] M.C. Wakeham, D. Frolov, P.K. Fyfe, R. van Grondelle, M.R. Jones, Acquisition of photosynthetic capacity by a reaction centre that lacks the Q_A ubiquinone; possible insights into the evolution of reaction centres? Biochim. Biophys. Acta, Bioenerg. 1607 (2003) 53–63.

[45] I.H.M. van Stokkum, T. Scherer, A.M. Brouwer, J.W. Verhoeven, Conformational dynamics of flexibly and semirigidly bridged electron donor–acceptor systems as revealed by spectrotemporal parametrization of fluorescence, J. Phys. Chem. 98 (1994) 852–866.

[46] Z. Otwinowski, W. Minor, Processing of X-ray diffraction data collected in oscillation mode, Methods Enzymol. 276 (1997) 307–326.

[47] J. Navaza, AMORE—Un automated package for molecular replacement, Acta Crystallogr. A 50 (1994) 157–163.

[48] G.N. Murshudov, A.A. Vagin, E.J. Dodson, Refinement of macromolecular structures by the maximum-likelihood method, Acta Crystallogr., D 53 (1997) 240–255.

[49] M.C. Wakeham (2004) PhD Thesis, University of Bristol.

[50] E.J. Bylina, C. Kirmaier, L. McDowell, D. Holten, D.C. Youvan, Influence of an amino-acid residue on the optical-properties and electron-transfer dynamics of a photosynthetic reaction center complex, Nature 336 (1988) 182–184.

[51] J. Breton, E.J. Bylina, C.Y. Youvan, Pigment organization in genetically modified reaction centers of Rhodobacter capsulatus, Biochemistry 28 (1989) 6423–6430.

[52] D. Beese, R. Steiner, H. Scheer, A. Angerhofer, B. Robert, M. Lutz, Chemically modified photosynthetic bacterial reaction centers-circular-dichroism, Raman resonance, low-temperature absorption, fluorescence and ODMR spectra and polypeptide composition of borohydride treated reaction centers from Rhodobacter spheroides R26, Photochem. Photobiol. 47 (1988) 293–304.

[53] J. Breton, Low temperature linear dichroism study of the orientation of the pigments in reduced and oxidized reaction centers of Rps. viridis and Rb. sphaeroides, in: J. Breton, A. Verméglio (Eds.), The Photosynthetic Bacterial Reaction Center, Structure and Dynamics, Plenum, New York, 1988, pp. 59–69.

[54] J. Breton, M.C. Wakeham, P.K. Fyfe, M.R. Jones, E. Nabedryk, Characterization of the bonding interactions of Q_B upon photoreduction via A-branch or B-branch electron transfer in mutant reaction centers from Rhodobacter sphaeroides, Biochim. Biophys. Acta, Bioenerg. 1656 (2004) 127–138.

[55] Q. Zhou, B. Robert, M. Lutz, Protein prosthetic group-interactions in bacterial reaction centers—Resonance Raman-spectroscopy of the reaction center of Rhodopseudomonas-viridis, Biochim. Biophys. Acta 977 (1989) 10–18.

[56] B. Robert, Resonance Raman studies of bacterial reaction centres, Biochim. Biophys. Acta 1017 (1990) 99–111.

[57] V. Palaniappan, D.F. Bocian, Resonance Raman-spectroscopic evidence for dielectric asymmetry in bacterial photosynthetic reaction centers, J. Am. Chem. Soc. 117 (1995) 3647–3648.

[58] C. Kirmaier, P.D. Laible, K. Czarnecki, A.N. Hata, D.K. Hanson, D.F. Bocian, D. Holten, Comparison of M-side electron transfer in Rb. sphaeroides and Rb. capsulatus reaction centers, J. Phys. Chem., B 106 (2002) 1799–1808.

[59] J. Breton, E. Nabedryk, J.P. Allen, J.A.C. Williams, Electrostatic influence of Q_A reduction on the IR vibrational mode of the 10a-ester C=O of H_A demonstrated by mutations at residues Glu L104 and Trp L100 in reaction centers from Rhodobacter sphaeroides, Biochemistry 36 (1997) 4515–4525.

[60] J. Breton, M. Bibikova, D. Oesterhelt, E. Nabedryk, Conformational heterogeneity of the bacteriopheophytin electron acceptor H_A in reaction centers from Rhodopseudomonas viridis revealed by Fourier transform infrared spectroscopy and site-directed mutagenesis, Biochemistry 38 (1999) 11541–11552.

[61] S. Krimm, J. Bandekar, Vibrational spectroscopy and conformation of peptides, polypeptides, and proteins, Adv. Protein Chem. 38 (1986) 181–364.

[62] J. Breton, C. Boullais, C. Mioskowski, P. Sebban, L. Baciou, E. Nabedryk, Vibrational spectroscopy favors a unique Q_B binding site at the proximal position in wild-type reaction centers and in the Pro-L209→Tyr mutant from Rhodobacter sphaeroides, Biochemistry 41 (2002) 12921–12927.

[63] L.M.P. Beekman, R.W. Visschers, R. Monshouwer, M. Heer-Dawson, T.A. Mattioli, P. McGlynn, C.N. Hunter, B. Robert, I.H.M. van Stokkum, R. van Grondelle, M.R. Jones, Time-resolved and steady-state spectroscopic analysis of membrane-bound reaction centers from Rhodobacter sphaeroides: comparisons with detergent-solubilized complexes, Biochemistry 34 (1995) 14712–14721.

[64] L.M.P. Beekman, I.H.M. van Stokkum, R. Monshouwer, A.J. Rijnders, P. McGlynn, R.W. Visschers, M.R. Jones, R. van Grondelle, Primary electron transfer in membrane-bound reaction centers with mutations at the M210 position, J. Phys. Chem. 100 (1996) 7256–7268.

[65] J.P. Ridge, M.E. van Brederode, M.G. Goodwin, R. van Grondelle, M.R. Jones, Mutations that modify or exclude binding of the Q_A ubiquinone and carotenoid in the reaction center from Rhodobacter sphaeroides, Photosynth. Res. 59 (1999) 9–26.

[66] M.E. van Brederode, F. van Mourik, I.H.M. van Stokkum, M.R. Jones, R. van Grondelle, Multiple pathways for ultrafast transduction of light energy in the photosynthetic reaction center of Rhodobacter sphaeroides, Proc. Natl. Acad. Sci. U. S. A. 96 (1999) 2054–2059.

[67] E.C. Kellogg, S. Kolaczkowski, M.R. Wasielewski, D.M. Tiede, Measurement of the extent of electron-transfer to the bacteriopheophytin in the M-subunit in reaction centers of Rhodopseudomonas-viridis, Photosynth. Res. 22 (1989) 47–59.

[68] A.L. de Boer, S. Neerken, R. de Wijn, H.P. Permentier, P. Gast, E. Vijgenboom, A.J. Hoff, High yield of B-branch electron transfer in a quadruple reaction center mutant of the photosynthetic bacterium Rhodobacter sphaeroides, Biochemistry 41 (2002) 3081–3088.

[69] C. Kirmaier, P.D. Laible, D.K. Hanson, D. Holten, B-side charge separation in bacterial photosynthetic reaction centers: nanosecond time scale electron transfer from H_B^- to Q_B, Biochemistry 42 (2003) 2016–2024.

[70] P.D. Laible, C. Kirmaier, C.S.M. Udawatte, S.J. Hofman, D. Holten, D.K. Hanson, Quinone reduction via secondary B-branch electron transfer in mutant bacterial reaction centers, Biochemistry 42 (2003) 1718–1730.

[71] L. Xiong, M. Seibert, A.V. Gusev, M.R. Wasielewski, C. Hemann, C.R. Hille, R.T. Sayre, Substitution of a chlorophyll into the inactive branch pheophytin-binding site impairs charge separation in Photosystem II, J. Phys. Chem., B 108 (2004) 16904–16911.